Characterization of high refractive index semiconductor films by surface plasmon resonance

Sergiy Patskovsky, Souleymane Bah, Michel Meunier, and Andrei V. Kabashin

Si-based surface plasmon resonance (SPR) in the Kretschmann–Raether geometry is considered as a platform for the optical measurement of high refractive index films. The implementation of the SPR effect becomes possible due to the relatively high index of refraction of Si compared to most materials. As examples we study the SPR responses for some important semiconductor-based films, including laser-ablated porous silicon and thin germanium films. Using SPR data, we determine the refractive indices of these films for different parameters (thickness and porosity) and ambiences. We also discuss novel SPR biosensor architectures with the use of these solid films.

OCIS codes: 240.6680, 120.4820, 310.6860.

1. Introduction

Surface plasmon resonance (SPR) is known as one of the leading technologies for the measurement of optical properties of thin films and interfaces,[1] as well as for biological and chemical sensing (see, e.g., Refs. 2–6). Having a resonant response to a dielectric constant of a medium in contact with the SPR-supporting metal (usually gold), SPR enables us to determine the refractive index or thickness of thin films with an extremely high sensitivity. SPR measurements are mainly implemented in the Kretschmann–Raether prism geometry to direct *p*-polarized visible light through a glass prism and reflect it from a thin gold film deposited on the prism.[7] The SPR effect manifests itself as a dip in the angular (or wavelength) dependence of the intensity of light reflected from the gold film. A combination of the resonant angle of incidence and wavelength appears to be resonantly linked to properties of the adjacent medium within a thin layer of 200–300 nm, corresponding to the probe depth (δ) of the plasmon-based evanescent wave in visible light. This enables us to effectively control the properties of ultrathin films on gold, both of inorganic and organic origin, by following the resonant angle,[2–4] wavelength,[5,6] or phase[8,9] of the reflected light.

Generally speaking, SPR technology has a limitation to a maximum refractive index that could be measured. This limitation comes from a fundamental condition of SPR production, implying the necessity of relative predominance of the refractive index of the coupling prism (n_p) over the effective refractive index of the ambience within the probe depth of the evanescent wave δ. It is clear that even for glass prisms made of high refractive index materials ($n_p \sim 1.7$–1.8), the SPR method can be used mostly with biological and some low refractive index films, whereas many important solid films having promising properties for biosensing or other applications appear to be out of the applicability of the method.

As a modification of SPR, we recently showed the feasibility for the realization of the SPR effect in infrared light by using a Si coupling prism instead of the glass one.[10–13] Although the basic properties of Si-based SPR were rather different compared with conventional glass-based SPR,[10,11] this approach showed very promising characteristics for sensing and potential miniaturization and/or integration of SPR devices. Due to a relatively high refractive index of the Si prism (3.525 for $\lambda = 1200$ nm), the proposed Si-based platform also makes possible the characterization of solid films of much higher refractive indices. We reason that this advantage can be employed to combine SPR with some important semiconductor-based films whose properties are promising for the improvement of the characteristics of SPR devices. In particular, the potential advantages of using these films in SPR include the photoelectric control of SPR

The authors are with the Department of Engineering Physics, Ecole Polytechnique de Montréal, Case Postal 6079, Succ. Centreville, Montréal, Québec H3C 3A7, Canada. S. Patskovsky's e-mail address is sergiy.patskovsky@polymtl.ca.

Received 27 January 2006; revised 29 March 2006; accepted 5 April 2006; posted 6 April 2006 (Doc. ID 67490).

0003-6935/06/256640-06$15.00/0

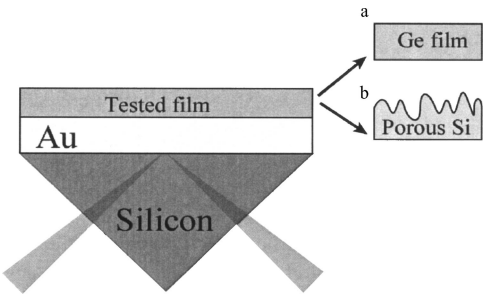

Fig. 1. Schematic of the experimental setup for the examination of properties of LAPS and Ge films.

characteristics and a simplification of the bioimmobilization step.

As a proof of the concept, we show the possibility of SPR characterization of some semiconductor-based films by the newly introduced Si-based technology. In particular, we examine the SPR response from nanoporous Si-based films, synthesized by a laser-ablation method,[14] and of thin Ge films. We also discuss how these films can be used in biosensor designs.

2. Experimental and Theoretical Methodology

We carried out a series of experiments in the Kretschmann–Raether prism arrangement consisting of a Si prism, a gold film, and a flow cell (empty or filled with deionized water, depending on whether the sensing medium is air or liquid), as shown schematically in Fig. 1. The SPR-supporting gold film was deposited by an electron beam evaporation technique on a 0.5 mm thick silicon wafer (FZ silicon, Silicon Quest, Santa Clara, California). The film thickness (35 nm) was optimized for experiments in the near-infrared (Ref. 10). The wafer with gold was then placed in the immersion contact with a base of a Si prism (Silicon Quest) by using a high refractive index immersion liquid (Cargille Laboratories, Cedar Grove, New Jersey) to provide a good optical and mechanical contact. The SPR coupling system was placed onto the rotary block of a Woollam variable angle spectroscopic ellipsometer (VASE) (J. A. Woollam, Lincoln, Nebraska) to allow for a very fine variation of the angular prism position with respect to the optical path of the ellipsometer. The system was illuminated by a monochromatic 1200 nm light and the light reflected from the coupling system was analyzed by a detector. The experiments were performed in the configuration of a fixed wavelength with the resolution of angular measurements at 0.01°.

In our study we examined the properties of porous silicon (PS) [Fig. 1(a)] and germanium films [Fig. 1(b)]. The films were deposited directly on the SPR-supporting gold. Scanning electron microscopy (SEM), atomic force microscopy (AFM), and x-ray diffraction (XRD) were used to examine the structural properties of the PS and germanium films. To quantify the porosity of semiconductor-based films, we used a method of specular x-ray reflectivity (SXRR), a modification of XRD, based on the measurements of the total external reflection of x rays from the films.[15] Details on these measurements can be obtained in Ref. 14.

To optimize the response of SPR, we also developed a theoretical framework on the basis of the surface plasmon model, which made possible a simulation of the SPR effect in multilayer systems. In our calculations the data for the dispersion characteristics of germanium were taken from the database of refractive indices[16] (Sopra SA, France) and corrected for thin films by direct ellipsometric measurements in an appropriate wavelength range (1100–1600 nm). The dispersion properties of gold in visible and IR light were taken from the data of Innes and Sambles[17] and Johansen *et al.*[18] The optical constants for Si were obtained from the approximation of experimental dependences reported by Herzinger *et al.*[19]

3. Results and Discussion

In our study, we used the Si-based SPR platform to examine optical properties of thin semiconductor-based films, which could potentially be integrated in the SPR biosensor to improve its characteristics. First, we tested PS films, fabricated by laser ablation.[14] Composed of a nanocrystalline skeleton (quantum sponge) immersed in a network of pores, this novel material is similar in many respects to conventional PS prepared by anodical etching.[20] However, in contrast to conventional PS, the laser-ablated films can be deposited on almost any arbitrary surface, including gold, facilitating the design of Si-based biosensors or optoelectronic devices. In addition, the laser-ablation approach enables us to avoid chemical contamination, typical for the anodical etching procedure, and to control the surface chemistry of the produced layers. Briefly, a Si wafer is illuminated by radiation from an excimer laser (e.g., KrF with a wavelength of 248 nm and a pulse length of 20 ns FWHM) in the helium gas, maintained at a residual pressure (0.02–10 Torr). Focused on the target at some incident angle, the radiation causes the ablation of material from the target, which expands perpendicular to the target surface. The material is then deposited on a rotated substrate and placed at some distance from the target to form a thin film of porous nanocrystalline Si (LAPS). The film thickness can reach several micrometers after a few thousand laser shots. As shown in Ref. 14, this method enables us to finely vary the porosity of the thin films from 25% to one exceeding 90% by a variation of the pressure of helium between 0.1 and 10 Torr. Details on the deposition procedure and the properties of the porous silicon films can be found in Ref. 14.

We deposited LAPS films on the SPR-supporting gold films under different pressures of residual helium gas. Figure 2 shows the typical SEM images of Si-based films on gold. One can see that the films had a porous structure, similar to conventional PS fabricated by anodical etching, while the porosity could be controlled by varying the parameters of laser ablation. In our tests, we used relatively thick films with the thickness (2–4 μm) much larger than the probe depth ($d > \delta$) of the SPR method.

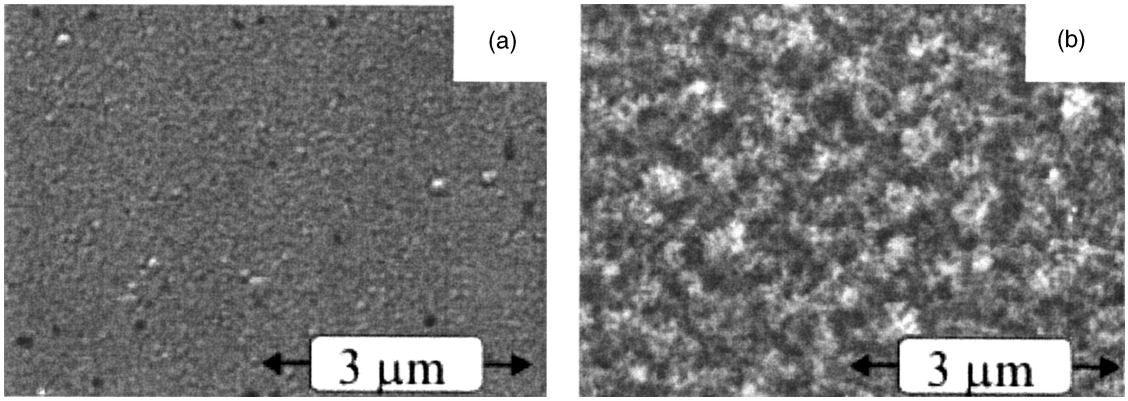

Fig. 2. SEM images of typical laser-ablated porous Si films with porosity of (a) 50% and (b) 90%. The porosity was measured by x-ray specular reflectivity.

Our experiments showed that the SPR effect can be implemented for a LAPS film of different porosities. As presented in Fig. 3(a), typical SPR reflectivity curves were relatively narrow, while the width of the dip depended on the porosity. In particular, the decrease of the film porosity from 74% to 38% led to the increase of the width from 0.2° to 1.2° FWHM. Figure 3(b) presents the dependence of the SPR angular dip on the film porosity. One can see that the decrease of the film porosity leads to a significant increase of the resonant angle. For example, the decrease of the film porosity from 74% to 38% resulted in an angle shift from 22° to 46°. This phenomenon is explained by an increase of the refractive index of the LAPS films when the porosity decreases.

SPR data can now be used to estimate the effective refractive index of LAPS films. As long as the typical structure size (the size of the Si crystals and pores) is much lower than the emission wavelength, the PS layers appear as an effective medium whose index of refraction has an intermediate value between the index of refraction of Si (structures) and that of the air (pores). In this case, the weight of the pore contribution is precisely the porosity. However, the precise determination of porosity is complicated by the fact that the nanocrystal-based skeleton is covered by SiO_2. The refractive index of such a structure depends on a combination of factors related to a relative percentage of the Si crystals, its compounds, and the air in the whole film volume. Since the conditions of SPR excitation are directly related to the refractive index of the medium contacting the gold film, SPR data can be used to precisely determine the effective refractive index of the LAPS films. Substituting the data on the angular positions of the SPR minima to Fresnel's formulas,[21] we can obtain values of refractive index for the films of different porosities, shown in Fig. 4 by a solid curve. The same figure (dotted curves) shows the estimations of the PS film porosity, provided the film is composed of a purely silicon skeleton, while the pores are filled by air or water (typical gas or biosensing conditions). In the latter estimation of n_{eff}, we used the Bruggeman effective medium approximation (EMA) theory,[22] in which the porosity and the refractive index are linked by the following formula:

$$f_m \frac{{n_{\mathrm{Si}}}^2 - {n_{\mathrm{eff}}}^2}{{n_{\mathrm{Si}}}^2 + 2{n_{\mathrm{eff}}}^2} + (1 - f_m)\frac{{n_m}^2 - {n_{\mathrm{eff}}}^2}{{n_m}^2 + 2{n_{\mathrm{eff}}}^2} = 0, \qquad (1)$$

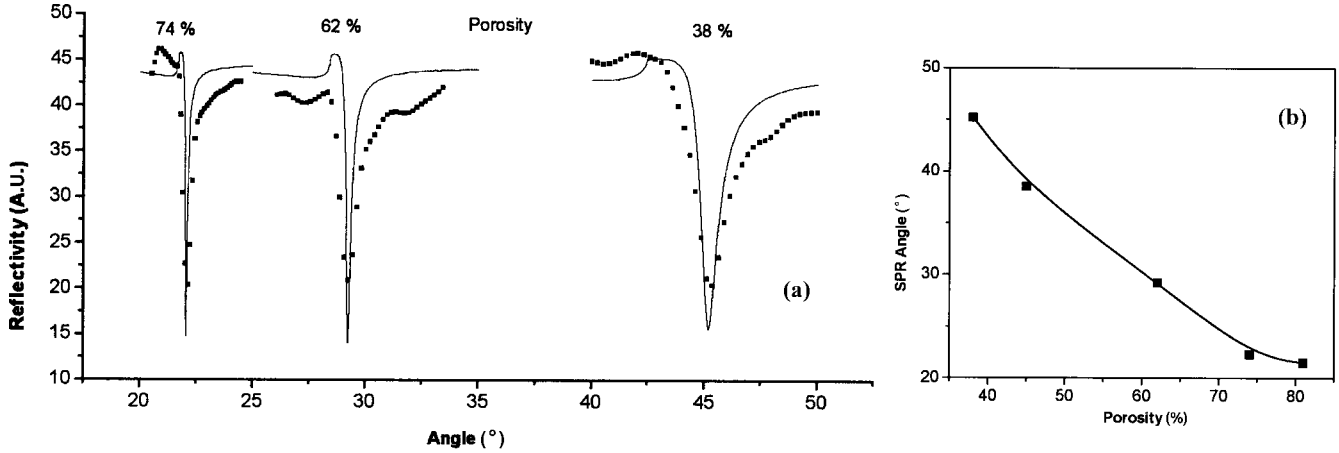

Fig. 3. (a) SPR reflectivity curves for PS films with different porosities. (b) SPR resonant angle as a function of porosity of PS films. Solid curve shows the extrapolation of experimental data.

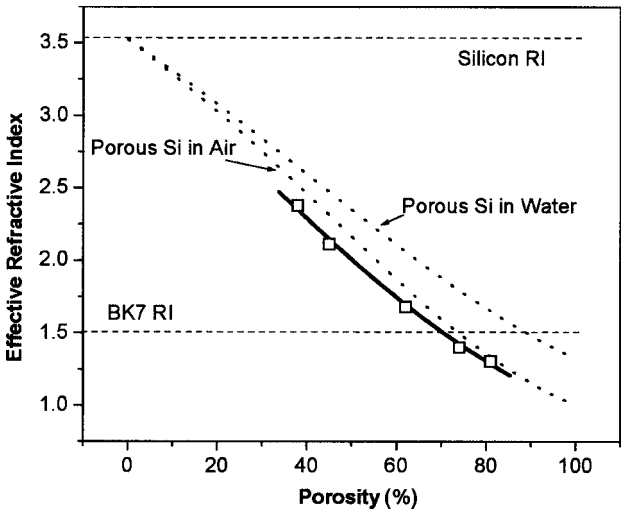

Fig. 4. Effective refractive index of laser-ablated porous Si determined from the analysis of experimental data (solid curve with squares). For comparison, the refractive index of porous Si calculated by the Bruggeman EMA theory in water and air is presented by dotted curves.

where n_{Si} is the refractive index of silicon, n_m is the refractive index of the host material, which is air or water for our case, and f_m is a volume fraction of the components.

As follows both from the experimental results and the theoretical calculations, the effective refractive index n_{eff} decreases as the film porosity increases. In particular, the increase of the porosity from 38% to 80% leads to a decrease of the refractive index from 2.4 to 1.4. Here, experimental data give slightly lower values of refractive index compared to theoretical ones. This discrepancy is probably explained by simplified considerations in the Bruggeman theory used for calculations of the refractive index.[22]

Thus we were able to reproduce the SPR effect for nanoporous Si-based films of various porosities. We reason that the combination of SPR with LAPS films gives attractive opportunities to improve the performance of the SPR biosensors. In particular, when used as a matrix for the immobilization of biological species, LAPS films enable us to simplify the bioimmobilization step. Indeed, the surface of Si and its compounds (SiO_2) is known as one of the best matrices for immobilization of different biological entities including enzymes, antibodies, receptors and/or ligands, and cells, while methods of bioimmobilizations on a Si-based surface are well elaborated and often much simpler compared with those for gold.[23,24] Furthermore, the spongelike structure of LAPS is characterized by a very large internal surface area (of the order of 100–1000 m^2/cm^3), which enables us to put much more biomaterial within the probe depth of the SPR method and thus increase the sensitivity of the SPR biosensor. We suppose that such a matrix must be especially effective in the case of small biological species such as small molecular weight proteins and drugs. In this case, the size of the pore openings can be controlled to fit the size of the species by variations in the laser-ablation procedure.

Second, we used the Si-based SPR platform to characterize the thin Ge films. This case is important for understanding how the plasmons are excited and damped in the presence of a thin absorbing semiconductor layer having a higher refractive index ($n_{Ge} = 4.35$) compared to the coupling material (Si) and quite different dispersion properties. Since the SPR effect gives an enormous field enhancement, this configuration is also interesting from the point of view of potential photoelectrical applications of SPR technology. Indeed, Ge still efficiently absorbs light in the region of Si transparency (1100–1500 nm). Since light absorption in semiconductors is accompanied by the photoexcitation of carriers, we can imagine the implementation of a Ge-based thin-film photoelectronic detector, based on measurements of plasmon wave-induced generation of carriers in the Ge film. As the first step in this direction, we examine conditions of SPR production when a thin Ge film is placed on SPR-supporting gold. Films of Ge (99.99%, Aldrich) were deposited on a Si wafer covered by gold by a technique of electron beam evaporation. The deposition was performed at a constant rate of 0.1 A/s under vacuum with residual air pressure of $P = 2 \times 10^{-6}$ Torr.

As in the case of LAPS, our experiments reported a possibility of the implementation of the SPR effect when the films of Ge covered gold. In general, the SPR reflectivity curves were broader for Ge compared to Si, while the width of the curves was very sensitive to the film thickness. As shown in Fig. 5(a), a slight increase of the thickness from 30 to 40 nm resulted in the increase of the width of the curves from 1.2° to 9° FWHM. This broadening was apparently related to a certain damping of a plasmon wave under its interaction with a semiconductor because of the presence of a nonzero imaginary part in the refractive index of Ge. The change of the film thickness also led to a significant shift of the SPR angle. In particular, the increase of the film thickness from 30 to 40 nm shifted the SPR minimum from 19° to 37°, as shown in Fig. 5(b). The coupling conditions could be satisfied up to the thickness of the Ge layer of approximately 55–60 nm, providing an almost glancing SPR angle (80°–85°).

It is clear that the realization of the SPR effect for Ge was possible due to a relatively large probe depth of surface plasmon wave in the near-IR range and the high refractive index of the silicon coupling prism.[10] Therefore SPR senses an effective refractive index n_{eff}, which is a combination of the high refractive index of the Ge film and a low refractive index of the ambience (air). Generally speaking, SPR enables us to precisely obtain the value of n_{eff}. Figure 4(b) shows a dependence of n_{eff}, derived from SPR measurements, on the thickness of the Ge film (solid curve). One can see that thicknesses larger than 30–35 nm lead to a drastic increase of the refractive index n_{eff} approaching values of 3. Approaching the refractive

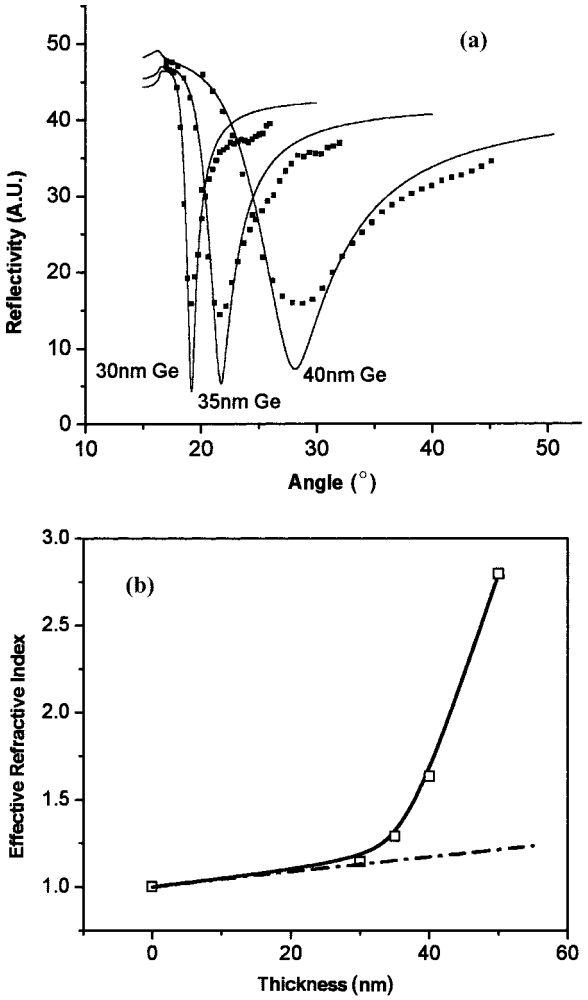

Fig. 5. (a) Angular SPR reflectivity curves for different thicknesses of Ge films on SPR-supporting gold. (b) Dependence of the SPR resonant angle on the thickness of Ge. Solid curve represents the extrapolation of experimental data; the dashed line represents the theoretical estimation using Eq. (2).

index of coupling Si (3.4) under thicknesses of approximately 55–60 nm, it becomes impossible to match the wavenumbers of the pumping light and surface plasmons. Note that the calculation of the effective refractive index by standard formulas can lead to incorrect values in the case of high refractive index Ge films. Indeed, let us consider a standard expression for the effective refractive index n_{eff}[18]:

$$n_{\text{eff}} = \frac{\int_0^\infty n(z)e^{-z/\delta}dz}{\int_0^\infty e^{-z/\delta}dz} = n_{\text{Ge}} + e^{-d/\delta}(n_m - n_{\text{Ge}}), \quad (2)$$

where d is the layer thickness, δ is the probe depth, z is the height above the metal surface, and n_m is the refractive index of air. A dotted curve in Fig. 4(b) shows the value of the refractive index obtained from this expression as a function of the Ge film thickness. As follows from Fig. 4 the formula is valid only for small thicknesses of the Ge film (<30 nm), whereas larger thicknesses lead to unrealistically small values of n_{eff}. In our opinion, the discrepancy of theoretical values is related to an incomplete description of the phenomenon by Eq. (2), since this formula does not take into account the influence of the Ge film on the penetration depth of surface plasmons.

Finally, it is important to note that the realization of SPR was possible for thicknesses of Ge up to 50–60 nm. Basically, thicknesses of 20–30 nm are already sufficient to satisfy minimal technological requirements to form an integrated thin-film Ge-based photodetector. Work on the implementation of such a SPR photodetector is now in progress. The results will be published in a future work.

4. Conclusions

Si-based surface plasmon resonance in the Kretschmann–Raether geometry has been used to characterize thin high refractive index semiconductor films (laser-ablated porous Si and Ge). Using SPR data, we determined the refractive indices of the LAPS films for different porosities and compared them with theoretical predictions. In addition, we determined the conditions of SPR implementation for Ge films, having a much higher refractive index compared to a coupling Si prism. We also discussed novel SPR biosensor architectures with the use of these solid films.

The authors thank Ludvik Martinu of the Department of Engineering Physics, Ecole Polytechnique de Montreal, for assistance with the experimental facilities. The authors also acknowledge the financial contribution from the Natural Science and Engineering Research Council of Canada and the Canadian Institute for Photonics Innovations (CIPI).

References

1. V. M. Agranovich and D. L. Mills, eds., *Surface Polaritons: Electromagnetic Waves at Surfaces and Interfaces* (North-Holland, 1982).
2. B. Liedberg, C. Nylander, and I. Lundstrum, "Surface plasmon resonance for gas detection and biosensing," Sens. Actuators B **4,** 299–304 (1983).
3. B. Liedberg, C. Nylander, and I. Lundstrom, "Biosensing with surface plasmon resonance: How it all started," Biosens. Bioelectron. **10,** i–ix (1995).
4. J. L. Melendez, R. Carr, D. U. Bartholomew, K. A. Kukanskis, J. Elkind, S. S. Yee, C. E. Furlong, and R. G. Woodbury, "A commercial solution for surface plasmon sensing," Sens. Actuators B **35,** 212–216 (1996).
5. L. M. Zhang and D. Uttamchandani, "Optical chemical sensing employing surface plasmon resonance," Electron. Lett. **23,** 1469–1470 (1988).
6. R. C. Jorgenson and S. S. Yee, "Fiber-optic chemical sensor based on surface plasmon resonance," Sens. Actuators B **12,** 213–220 (1993).
7. E. Kretschmann and H. Raether, "Radiative decay of nonradiative surface plasmons excited by light," Z. Naturforsch. A **23,** 2135–2136 (1968).
8. A. V. Kabashin and P. I. Nikitin, "Surface plasmon resonance

interferometer for bio- and chemical-sensors," Opt. Commun. **150,** 5–8 (1998).
9. A. N. Grigorenko, P. I. Nikitin, and A. V. Kabashin, "Phase jumps and interferometric surface plasmon resonance imaging," Appl. Phys. Lett. **75,** 3917–3919 (1999).
10. S. Patskovsky, A. V. Kabashin, M. Meunier, and J. H. T. Luong, "Properties and sensing characteristics of surface plasmon resonance in infrared light," J. Opt. Soc. Am. A **20,** 1644–1650 (2003).
11. S. Patskovsky, A. V. Kabashin, M. Meunier, and J. H. T. Luong, "Surface plasmon resonance sensor on a silicon platform," Sens. Actuators B **97,** 409–414 (2004).
12. S. Patskovsky, A. V. Kabashin, M. Meunier, and J. H. T. Luong, "Silicon-based surface plasmon resonance sensing with two surface plasmon polariton modes," Appl. Opt. **42,** 6905–6909 (2003).
13. S. Patskovsky, A. V. Kabashin, M. Meunier, and J. H. T. Luong, "Multi-layer Si-based surface plasmon resonance structure for absorption sensing," Anal. Lett. **36,** 3237–3246 (2003).
14. V. Kabashin, J.-P. Sylvestre, S. Patskovsky, and M. Meunier, "Correlation between photoluminescence properties and morphology of laser-ablated Si/SiO_x nanostructured films," J. Appl. Phys. **91,** 3248–3254 (2002).
15. L. G. Parratt, "Surface studies of solids by total reflection of X-rays," Phys. Rev. **95,** 359–369 (1954).
16. Data may be retrieved at http://www.sopra-sa.com/more/database.asp.
17. R. A. Innes and J. R. Sambles, "Optical characterization of gold using surface plasmon-polaritons," J. Phys. F **17,** 277–287 (1987).
18. K. Johansen, H. Arwin, I. Lundström, and B. Liedberg, "Imaging surface plasmon resonance sensor based on multiple wavelengths: Sensitivity considerations," Rev. Sci. Instrum. **71,** 3530–3538 (2000).
19. C. M. Herzinger, B. Johs, W. A. McGahan, J. A. Woollam, and W. Paulson, "Ellipsometric determination of optical constants for silicon and thermally grown silicon dioxide via a multi-sample, multiwavelength, multiangle investigation," J. Appl. Phys. **83,** 3323–3336 (1998).
20. E. V. Astrova and V. A. Tolmachev, "Effective refractive index and composition of oxidized porous silicon films," Mater. Sci. Eng. B **69,** 142–148 (2000).
21. E. Hecht, *Optics,* 2nd ed. (Addison–Wesley, 1987).
22. D. A. G. Bruggeman, "Calculation of various physical constants of heterogeneous substances. I. Dielectric constant and conductivity of mixtures of isotropic substances," Ann. Phys. **24,** 636–664 (1935).
23. J. M. Brockman, A. G. Frutos, and R. M. Corn, "A multi-step chemical modification procedure to create DNA arrays on gold surfaces for the study of protein-DNA interactions with surface plasmon resonance imaging," J. Am. Chem. Soc. **121,** 8044–8051 (1999).
24. M. Thust, M. J. Schoning, S. Frohnhoff, R. Arens-Fischer, P. Kordos, and H. Luth, "Porous silicon as a substrate material for potentiometric biosensors," Meas. Sci. Technol. **7,** 26–29 (1996).